# Partial-Shading Assessment of Photovoltaic Installations via Module-Level Monitoring

## Preprint


C. Deline and S. MacAlpine
*National Renewable Energy Laboratory*

A. Hanson, J. Stauth, and C. Sullivan
*Dartmouth College*



*Presented at the 40th Photovoltaic Specialist Conference (PVSC)*
*Denver, Colorado*
*June 8–13, 2014*



**NREL is a national laboratory of the U.S. Department of Energy**
**Office of Energy Efficiency & Renewable Energy**
**Operated by the Alliance for Sustainable Energy, LLC**

This report is available at no cost from the National Renewable Energy Laboratory (NREL) at www.nrel.gov/publications.

**Conference Paper**
NREL/CP-5J00-63765
February 2015

Contract No. DE-AC36-08GO28308

This report is available at no cost from the National Renewable Energy Laboratory (NREL) at www.nrel.gov/publications.

Available electronically at http://www.osti.gov/scitech

Available for a processing fee to U.S. Department of Energy and its contractors, in paper, from:

U.S. Department of Energy
Office of Scientific and Technical Information
P.O. Box 62
Oak Ridge, TN 37831-0062
phone: 865.576.8401
fax: 865.576.5728
email: mailto:reports@adonis.osti.gov

Available for sale to the public, in paper, from:

U.S. Department of Commerce
National Technical Information Service
5285 Port Royal Road
Springfield, VA 22161
phone: 800.553.6847
fax: 703.605.6900
email: orders@ntis.fedworld.gov
online ordering: http://www.ntis.gov/help/ordermethods.aspx

*Cover Photos: (left to right) photo by Pat Corkery, NREL 16416, photo from SunEdison, NREL 17423, photo by Pat Corkery, NREL 16560, photo by Dennis Schroeder, NREL 17613, photo by Dean Armstrong, NREL 17436, photo by Pat Corkery, NREL 17721.*

NREL prints on paper that contains recycled content.

# Partial-Shading Assessment of Photovoltaic Installations via Module-Level Monitoring

Alex Hanson, Chris Deline, *Member, IEEE*, Sara MacAlpine, Jason Stauth, *Member, IEEE* and Charles R. Sullivan, *Senior Member, IEEE*

*Abstract*— **Distributed Maximum Power Point Tracking (DMPPT) is a topic of much interest in improving photovoltaic (PV) system performance. This study uses measured performance data at the module level for 542 PV systems to estimate lost system performance due to partial shade. Because each of the monitored systems is equipped with module-level DC power optimizers, an estimate is made of the overall system shading loss and the performance improvement that the system has received from this use of DMPPT. The estimate of shade extent and performance improvement predicted by this approach is verified experimentally against a system that has site survey images, and measured production with and without module-level electronics.**

**Summary data for this analysis across 542 systems find an average power loss of 8.3% due to partial shading, which would have increased to 13% were the systems not equipped with panel-level optimizers. It is estimated that on average, 36% of the power lost from partial shading has been recovered through use of module-level DC power electronics.**

***Index Terms*— DC power optimizer, distributed power electronics, DMPPT, partial shading, PV system performance.**

## I. Introduction

The use of distributed electronics in photovoltaic (PV) systems provides the ability to improve performance under mismatched operating conditions. Partial shading can lead to annual performance losses of 10%–20% or more in residential installations [1], due to both reduced irradiance on the PV modules, and mismatch loss due to irradiance differences throughout the system. Module-level power electronics such as microinverters or DC power optimizers have been shown to reduce mismatch in systems, recovering 30%–40% of the power lost due to partial shading [1–3]. However, the performance benefit of using distributed maximum power-point tracking (DMPPT) depends on the extent of mismatch in the PV system [4], along with details of the layout and topology of the system [5]. Although analyses of module-level electronics performance improvement have been conducted based on estimated or simulated PV system mismatch [1–6, 20-24], field verifications of these electrical models have been limited, or only demonstrated in small testbeds [25]. Often, a site visit is required to obtain information about the system layout and nearby shading obstructions through photographic imaging [7, 8].

Field current-voltage (IV) curves have been measured for aged, mismatched PV systems without any shading [9], giving an indication of inherent mismatch that can be expected in PV installations. This *inherent mismatch* is due to relatively permanent features such as age, damage, and process variation. Mismatch from *partial shading* can also be estimated over large areas by ray-tracing analyses of the built environment [10–12].

We present an additional method to estimate the mismatch within a system: analysis of the system's module-level performance data. Prior analyses at the utility meter level have estimated performance relative to expected performance in a large number of systems [13–15]. However, finer time-resolution data at the module-level are required to determine the amount of mismatch within a PV system and the potential for recovery from the use of distributed power electronics.

Rather than using specific module-level data monitoring equipment, the distributed electronics themselves can be used to report performance data, typically at 1-min time intervals and at the module level. Currently, most commercially available DMPPT devices provide the capability of data reporting at the module level and report real-time performance to a central database. The DC power optimizer manufacturer Tigo Energy operates such a database using the PV 2.0 data standard, with a subset available for academic research [16], which was used here.

Although systems already equipped with DMPPT do not allow a direct comparison between performance with and without the use of per-panel power electronics, the reporting capabilities of the module-level electronics provide some indication of the amount of external (i.e., partial shading) and inherent mismatch within the PV system.

Manuscript received May 29, 2014. This work was supported in part by the U.S. Department of Energy under Contract No. DE-AC36-08-GO28308 with the National Renewable Energy Laboratory and with a U.S. Department of Energy SunShot Incubator 6 award to Tigo Energy. This work was also supported in part by the National Science Foundation under grant number 1309905.

C. Deline is with the National Renewable Energy Laboratory, Golden, CO 80401 USA (phone: 303-384-6359; e-mail: chris.deline@nrel.gov).

A. Hanson was an undergraduate with the Thayer School of Engineering at Dartmouth, Hanover, NH 03755. He is now in the graduate school program, Massachusetts Institute of Technology, Boston, MA 02139 USA (e-mail: Alex.J.Hanson.14@dartmouth.edu).

S. MacAlpine is with the National Renewable Energy Laboratory, Golden, CO 80401 USA (e-mail: sara.macalpine@nrel.gov).

J. Stauth is with the Thayer School of Engineering at Dartmouth, Hanover, NH 03755 USA. (e-mail: jason.t.stauth@dartmouth.edu).

C. Sullivan is with the Thayer School of Engineering at Dartmouth, Hanover, NH 03755 USA. (e-mail: charles.r.sullivan@dartmouth.edu).

One caution in the use of module-level DC power electronics data to estimate mismatch within PV installations is that PV installations with installed DMPPT may not be representative of the wider community of residential or commercial systems. For instance, DMPPT may be more likely to be implemented on rooftops with greater than average amounts of shading or tilt/azimuth variation. However, analysis could still be conducted for the population of systems that are equipped with DMPPT to determine whether they provide a net advantage to these systems.

### A. *Details of the Monitored Systems*

Performance data are available for 542 installations totaling 5.2 MW of capacity in 26 different countries. The majority of installations (404) are smaller installations below 10 kW. Only 26 installations are 25 kW or above in size (Table I).

TABLE I. DISTRIBUTION OF PV SYSTEM SIZES IN THE TIGO ACADEMIC DATABASE

| System size between (kW) | # Systems |
|---|---|
| 0 | |
| 2.5 | 35 |
| | 160 |
| 5 | |
| | 209 |
| 10 | 93 |
| 15 | |
| | 19 |
| 25 | 17 |
| 50 | 5 |
| 100 | 4 |
| 400 | |

Each system in the database is equipped with Tigo Energy's DC power optimizers, which provide module-level peak-power tracking (MPPT) and monitoring. These optimizers are high-efficiency buck DC-DC converters, which allow individual panels within a series string to operate at their own independent MPPT, reducing mismatch losses (Fig. 1).

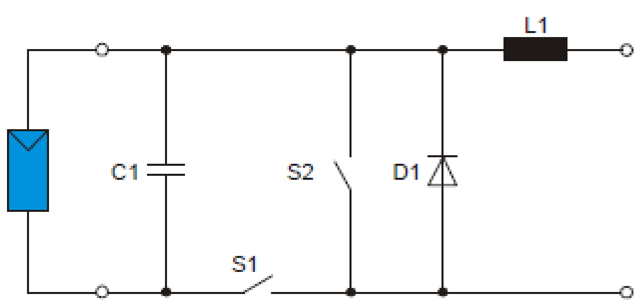


Fig. 1: Synchronous buck converter similar to that used in the Tigo MM-ES module-level converter [26]

The Tigo database contains various types of system- and module-level information including power, voltage, and temperature. For this method, only module-level DC power is required to assess partial-shading losses for a given system. Throughout this analysis, it is assumed that the Tigo DC power optimizers are correctly peak-power tracking the PV module they are connected to.

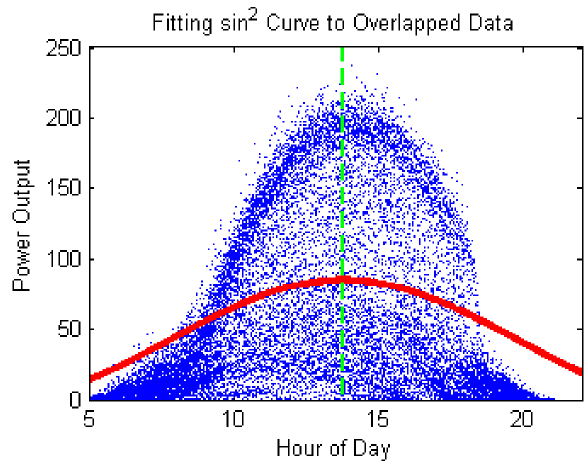


Fig. 2: Example of modular grouping analysis. A module's power data are overlaid on a single day (blue) and fit with a $\sin^2$ curve (red). The daily peak (green) for each module is used to determine its group assignment with other modules.

## II. PERFORMANCE ANALYSIS METHOD

To quantify the effect of partial shading on a solar array, we define a Shading Index as the actual energy output of an array over a given time period $E_{actual}$ divided by the estimated energy of the array had there been no partial shading $E_{unshaded}$:

$$\textit{Shading Index} = 1 - \frac{E_{actual}}{E_{unshaded}} \tag{1}$$

The Shading Index is a scalar indication of the extent of shading for various systems in the dataset. Note that all systems in the dataset are already equipped with per-panel Tigo devices, so the Shading Index naturally accounts for any partial-shade performance benefit provided by DMPPT.

$E_{actual}$ can be obtained directly by integrating the modules' output power over time. Estimating the unshaded production of a system $E_{unshaded}$ requires comparison of individual modules' production relative to the system production. The calculation consists of four steps: (1) identifying and segregating system subgroups with different physical orientations, (2) identifying times when the entire array is most clearly unshaded, (3) applying a correction for inherent module mismatch using data from unshaded periods, and (4) computing estimated unshaded energy outputs for each module at each time point. The following sections will explain the implementation of each step.

### A. *Orientation Grouping Identification*

To account for groups of panels oriented differently in a single system, each module is inspected for its performance vs time of day. Each data point for a given module is superimposed on a single 24-hour timescale, and a $sin^2$ function is then fit to the performance data to determine the offset of the production peak with respect to noon (see Fig. 2):

$$\text{Offset model} = \bar{P}_{modX} \sin^2(\pi t - \Delta t_X) \tag{2}$$

where $\bar{P}_{modX}$ is the best fit amplitude of module X's DC power production over all time and $\Delta t_X$ is the time offset of module X's peak production, in units of fractional days. In cases

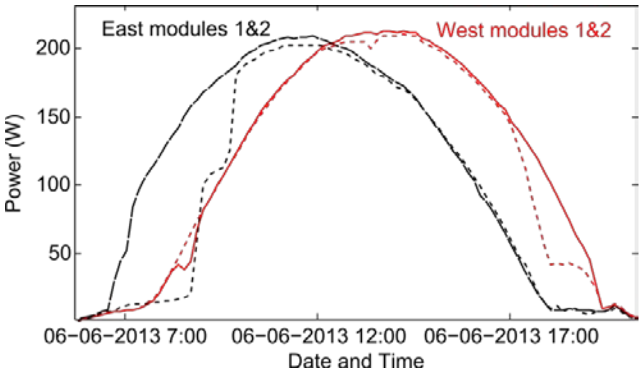


Fig. 3: System with different orientation groups, showing some modules angled slightly to the east, and some slightly to the west. East modules peak at 11:30 AM whereas West modules peak at 2:00 PM. Both orientations include partially shaded modules.

where $\Delta t_X$ varies from panel to panel by more than 1.5 hour, the panels are separated into independent groups to correctly identify mismatch and partial shading. An example of this type of variation is shown in Fig. 3. Only azimuth orientation was considered in this approach; variation in tilt was not investigated because tilt mismatch would not be discernable from partial-shading mismatch in the general case.

### B. *Inherent Mismatch - Module Performance Index*

To identify inherent differences in module performance, we seek examples of "unshaded" time points in the data. These are times of low standard deviation between panels where the entire array appears to either be unshaded, or uniformly shaded due to clouds. Times with partial shading should exhibit a wider variation in module power, whereas times with no shading should only exhibit the (much smaller) variations due to such factors as module soiling and aging. During these unshaded times, average inherent differences between module performance could be calculated.

Finding appropriately unshaded points to assess these inherent differences is somewhat difficult. In this work, the following method is employed. Unshaded time points were identified by their low inter-module Coefficient of Variation ($C_V$):

$$C_V(t) = \sigma_t / \bar{P}_t \qquad (3)$$

where $\sigma_t$ and $\bar{P}_t$ are the standard deviation and mean power across modules, respectively, at time *t*. Early-morning and late-evening times were excluded from consideration, as were time points with abnormally low $\bar{P}_t$. The time points with the lowest 1% $C_V$ were selected to represent module performance under equivalent (i.e., unshaded) illumination. (This is a somewhat arbitrary cutoff, but was found to generally exclude shaded points). The power at these *n* points was normalized by the array median power $\tilde{P}_t$ at time *t*, and averaged over all *n* time points to obtain a Performance Index (*PI*) for each module:

$$PI_X = \frac{1}{n}\sum_{t=1}^{n} \frac{P_{modX,t}}{\tilde{P}_t} \qquad (4)$$

The Performance Index represents a module-to-module comparison under equivalent illumination. Values over 1 indicate that a given panel performs, on average, better than the median. The *PI* of a given module is used in calculating its expected unshaded production, with higher-rated modules expected to produce more power under equivalent illumination. Typical *PI* values were found to be between 0.95 and 1.05, indicating less than 5% variation of module performance during unshaded conditions. In a few installations, large PI values resulted because different-sized modules were used in the same series string.

### C. *Estimated Unshaded Module Performance*

Estimated unshaded module performance is calculated for module X by multiplying the *PI* of module X by the maximum production of any module at each time step. The unshaded estimate, then, is simply the output power of the best-performing panel, scaled to account for inherent mismatch. This method assumes that at least one module at any given time is unshaded.

$$P_{modX,t,unshaded} = PI_X * \max(P_t) \qquad (5)$$

This analysis method will not account for shading experienced by the entire system; it is only sensitive to *partial-shading mismatch* within the system. This is a useful property in evaluating the performance benefit of DMPPT because DMPPT can *only* recover power losses attributable to mismatch. The estimated unshaded production is illustrated in Fig. 4 which compares the production of all modules in a system against the theoretical unshaded production (dark black line).

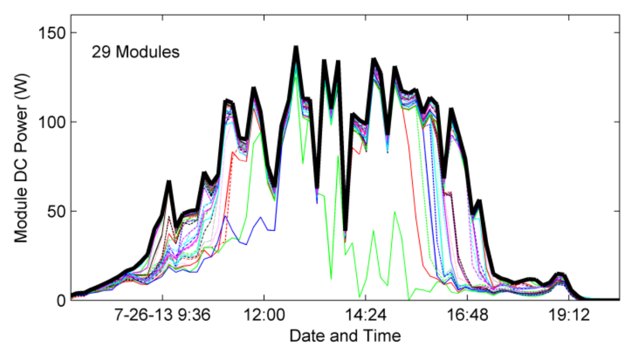


Fig. 4: Measured power for one system for one day of operation. Most modules track the maximum value (black) well. The Performance Index (PI) is computed from a module's average performance against the median during unshaded times. Unshaded theoretical performance for a module is equal to the maximum DC power at any time, adjusted by that module's PI.

### D. *"Diode" Mismatch Estimation*

As mentioned before, the module-level power data analyzed here come from systems with module-level DC power electronics attached. Therefore, we have no measured performance data for a conventional system to compare against. The module-level data can be adjusted in a rudimentary fashion to try to replicate the action of bypass diodes in a conventional system.

In a conventional PV system, partial shade on a module can result in that module's bypass diodes shorting out a portion of the module, zeroing out the power contribution from that submodule. This will occur if the irradiance on a particular module is significantly lower than on the rest of the system, because module currents must be matched in a conventional series-connected PV system.

This effect is replicated in the "Diode"' model case (Fig. 5), which assumes that a module's power production is zero during times that $P_{modX,actual}$ is 5% below the median module production. This is a gross simplification that likely over-states shading loss. A quick justification of this 5% cutoff value is that in modern silicon modules, $I_{sc}$ values are only 5-6% above the module's $I_{mp}$. In systems without DMPPT, shading a module by an amount of more than 5% will cause that module's $I_{mp}$ to drop below the Isc of the rest of the unshaded modules. In order to preserve current continuity, the shaded module's bypass diode must operate. Of course, this crude approximation does not account for shade covering only a portion of the module, and assumes that the number of shaded modules in a given string is small. Field results and additional simulations will however provide a verification of this approach in Section III.

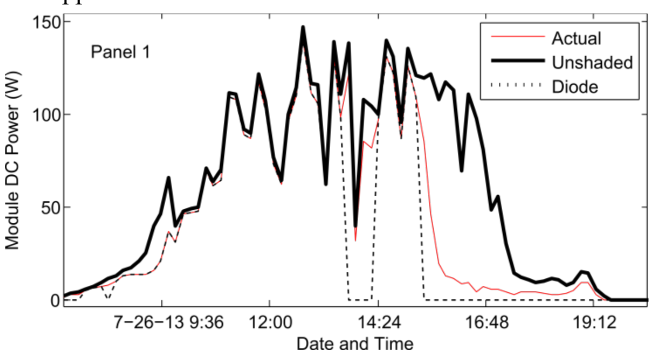


Fig. 5: Plot of actual and estimated unshaded power output for a single module in one system showing shaded times (when actual and unshaded diverge) and unshaded times (when they overlap). "Diode" case assumes zero module production if the actual module-level production is 5% below the system median.

### *E. More Detailed "Diode" Simulation*

To assess the accuracy of the simple "Diode" estimate, more detailed electrical simulations were conducted for a subset of available systems, based on previous simulation work [18]. Typical PV production models use meteorological data (irradiance, temperature) as inputs to estimate the resulting system production on an hourly basis. In our case, module-level power data were used as a substitute for module-level irradiance values at each time step. Given a spatial and temporal distribution of module power values, PV system production was estimated for different assumptions of system electrical configuration. For the case of module-level electronics, individual module power is summed to generate total system DC production. A more complicated case is for the use of string-level inverters, where module mismatch leads to a non-convex IV curve at the system level. The maximum of this system-wide curve is taken at each time step, assuming perfect MPPT tracking accuracy of the string inverter. This is a more robust method than the cruder "Diode" SI approximation above, and provides some estimates of uncertainty in the main method's approach.

## III. Model and Experimental Results

Plots of the above implementation (e.g., Figs. 4 and 5) illustrate that the algorithm gives predictions that would match a human or intuitive approach to the data. Times that were obviously shaded are correctly identified as shaded, and times that appeared to be unshaded are likewise appropriately identified.

With the estimated energy that panels would output under unshaded conditions, and the actual total energy output of the panels, the Shading Index *SI* was computed for each system by summing the actual and theoretical unshaded production of all modules in the system:

$$SI = 1 - \frac{\sum P_{modX,actual}}{\sum P_{modX,unshaded}} \qquad (6)$$

This Shading Index can be calculated for the actual production data, providing a value for each system equipped with module-level electronics. Alternatively, the "Diode" simulated results can be used instead of actual production data to make an estimate of what the Shading Index would be were the system deployed without DMPPT. The entire database of available systems was analyzed and the Shading Index values are reported in Fig. 6.

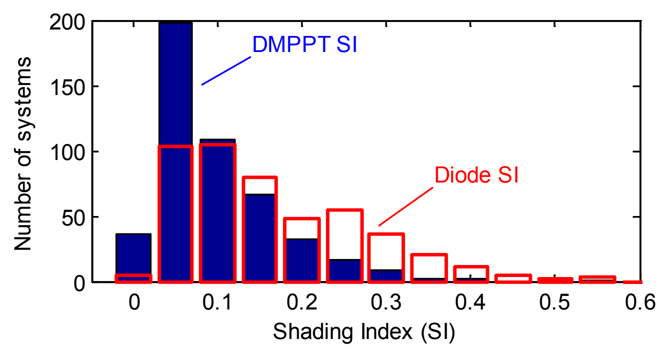


Fig. 6: Analysis of the shading index *SI* for each of the systems in the Tigo academic portal database. Median energy loss due to shading-induced mismatch was 8.3%. The "Diode" case models conventional PV system behavior and shows a median 13% shading loss, but a wider distribution.

### *A. Benchmarking of Shading Assessment*

Some verification of the above shade assessment method is possible by comparing the predicted shading index (SI) with on-site survey data collected on one of the systems in the database. This system (Fig. 7) is a residential system for which experimental measurements have been collected since 2011. The system is rated at 2.9 kW, and consists of two series strings of seven modules, each rated at 210 W. Additional detail on the system is provided in [17]. Site-survey data was collected using a SunEye imaging device, which estimates the monthly and annual irradiance reduction due to nearby shade obstructions. The site survey indicated monthly shading values from 10% to 45%, with an annual irradiance loss of 20% expected. The site survey is not directly comparable to our performance-based Shading Index; it is sensitive to uniform shading across the entire system, while our performance-based method is only sensitive to partial shading mismatch. The site survey also does not account for the performance benefits of DMPPT. However, if we do choose to compare the site survey with the performance-based method, the "Diode" modeled behavior would be the closest match.

Fig. 7: Photograph of the 2.8 kW, two-string PV system used to benchmark this method.

Figure 8 shows a comparison of the site-survey data with the performance-based Shading Index over 9 months of module-level performance data that were available. The overall annual Shading Index for the "Diode" case was 16%, compared with the 20% shading loss determined from the on-site shading survey. This is a slight under-prediction, again because the method is unable to detect total shading on a system, only partial shading. The module-level SI data suggest even lower partial shading loss of 11% because of the added benefit of DMPPT in reducing mismatch.

### B. *Benefits of DMPPT in Mismatched Systems*

DC performance data were monitored for the same system for a period of three years. In the initial two years, the system was configured in a conventional manner, with two parallel strings of modules connected to a single string inverter input. For the third year, the system was equipped with Tigo module-level DC-DC power optimizers. Therefore, a before-and-after comparison can be made for the same system with and without DMPPT.

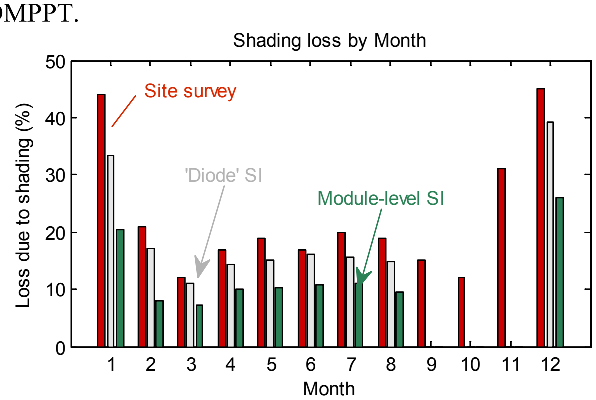


Fig. 8: Comparison of site-survey shading-loss estimate (Red bars) with performance-based Shading Index (Green bars) based on 9 months of module-level performance data. "Diode" Shading Index (gray) reflects the increased shading loss in a conventional system without DMPPT.

To account for differences in meteorological conditions, a separate data collection system was deployed in addition to the Tigo module-level measurements, monitoring module temperature, plane-of-array irradiance, and DC system voltage and current. The DC system performance was then corrected for temperature and irradiance. The performance ratio [19], corrected in this way, is shown in Fig. 9. On an annual basis, this temperature and irradiance corrected performance is 5.8% higher with the DMPPT than without. Many months showed a strong improvement in performance regardless of shade extent. However, some months showed little to no production improvement. Some of this monthly variation may be due to measurement uncertainty in temperature and irradiance, as well as variation in weather from year to year.

Turning to the measured module-level performance in the database, this system has a DC production with DMPPT of 1580 MWh over 9 months. This is 5.9% greater than the estimated "Diode" performance of 1492 MWh, showing a close match with the above before-and-after measurements.

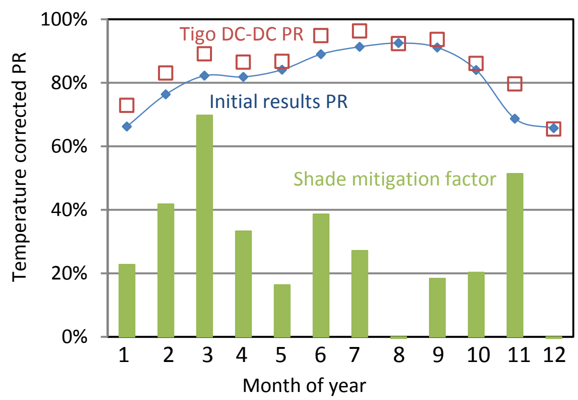


Fig. 9: Monthly Performance Ratio of a partially shaded residential system for three years. Years 1 and 2 (Blue diamonds) were without DMPPT. Year 3 (red squares) is with DMPPT. PR is normalized for temperature and irradiance. Green bars indicate monthly shade mitigation due to the DMPPT, average = 29%.

The energy improvement from module-level electronics can also be stated as a fraction of the total estimated loss from shade, based on the site survey. This "Shade Mitigation Factor" is represented by the green bars in Fig. 9. Again, there is a large variation in this factor, due to both measurement uncertainty in the shading site survey itself, and the before-and-after performance measurements for this system. The monthly shade mitigation value varies from 0% to 70%, with an average annual value of 29% of the expected shading loss recovered by DMPPT. This measured annual shade recovery value is close to prior simulations for this same system, which predicted 35% annual shade recovery [17].

To compare with the measured shade mitigation factor of 29% for this system, our estimated performance analysis method can be used to compute the same value. This requires a comparison between the annual system energy production using the three metrics we have developed: actual measured energy using DMPPT, estimated unshaded production, and estimated production for the "Diode" case. The Shade Mitigation Factor is calculated as follows:

$$SMF = \frac{\sum P_{actual} - \sum P_{Diode}}{\sum P_{unshaded} - \sum P_{Diode}} \quad (7)$$

By applying the above calculation to measured module-level data and estimated "Diode" and "Unshaded" production from this system we find an annual SMF value of 32%. This is close to both the experimental value (29%) and prior simulation values (35%).

The same process is applied to each system in the database with at least four months of production data, resulting in a calculation of 472 Shade Mitigation values. A contour plot is shown in Fig. 10, indicating a median system SMF value of 36%. Shade Mitigation values were found as high as 60% for systems with apparent tilt mismatch, or persistent shading even at noontime.

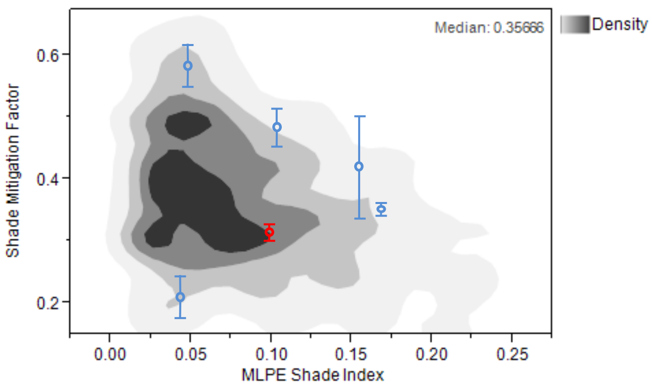


Fig. 10: Shade Mitigation Factor for all systems in the Tigo database. Median SMF value: 36%. Datapoint (red): validated system showing SMF of 29% - 32%. (Blue): Detailed simulation of 'Diode' performance for five additional systems showing difference between simulated and 'Diode' case.

### C. *"Diode" Estimation Validated with Detailed Simulation*

Figure 10 includes multiple validated systems where the "Diode" performance is simulated in detail, as described in II.E. The uncertainty error bars indicate the difference between simplified method and detailed simulation. Although the "Unshaded" response is still approximated from module-level performance rather than measured from a site survey, the more-accurate diode simulation provides greater certainty in a system's calculated Shade Mitigation Factor. For the five systems validated in this way, SMF values differed from the original method by less than 8% in all but one instance. This suggests that the method is relatively accurate in a majority of instances.

## IV. Conclusion

A database of module-level PV performance was analyzed to extract details of mismatch from external sources such as partial shading. A method to estimate the unshaded power of each system, and therefore, the expected power loss from partial shading was developed and benchmarked for a system with available site-survey data. Some difference exists between the two shading-loss estimates, partly due to differences in what each is measuring.

The performance benefit of DMPPT was investigated for a system before and after it was equipped with Tigo module-level electronics. An annual performance increase of 5.8% was measured following installation of the module-level electronics, which translates to a recovery of around 30% of the shading losses in the system. This is comparable to prior estimates of performance benefit in residential systems, and verified in this paper by further simulations using module-level performance data.

Analysis of all systems in the database indicated a median shading loss of SI = 8.3% due to partial shading, which increases to 13% for the "Diode" case. A median Shade Mitigation Factor of 36% was calculated for all systems and was validated by additional simulations of five separate installations.

The cost effectiveness of distributed maximum power-point tracking depends on the specifics of the installation and the marginal cost of the distributed electronics. The performance improvements shown above provide a technical basis for system owners and installers to properly assess the advantages of this type of DMPPT product.

## Acknowledgement


This work was supported by the U.S. Department of Energy under Contract No. DE-AC36-08-GO28308 with the National Renewable Energy Laboratory. This work was supported by a SunShot incubator award to Tigo Energy and by the National Science Foundation under grant number 1309905. Special thanks to Tigo Energy for access and technical support on the Tigo Energy Academic Data Portal.


## References


[1] C. Deline, J. Meydbray, M. Donovan, J. Forrest, "Photovoltaic Shading Testbed for Module-Level Power Electronics," NREL technical report NREL/TP-5200-54876, 2012

[2] C. Podewils, M. Levitin, "Hidden powers," Photon Magazine, November 2010

[3] S. MacAlpine, M. Brandemuehl, R. Erickson, "Characterization of Power Optimizer Potential to Increase Energy Capture in Photovoltaic Systems Operating Under Nonuniform Conditions," IEEE Transactions on Power Electronics **28**, pp. 2936-2945. 2013

[4] C. Deline, B. Marion, J. Granata, S. Gonzalez, A Performance and Economic Analysis of Distributed Power Electronics in Photovoltaic Systems. NREL Report No. TP-5200-50003. Golden, CO: National Renewable Energy Laboratory, December 2010.

[5] C. Deline, S. MacAlpine, "Use Conditions and Efficiency Measurements of DC Power Optimizers for Photovoltaic Systems", IEEE Energy Conversion Congress and Expo (ECCE) 2013 DOI: 10.1109/ECCE.2013.6647346

[6] C. Olalla, C. Deline, D. Maksimovic, "Performance of Mismatched PV Systems with Submodule Integrated Converters," IEEE Journal of Photovoltaics **4** pp. 396-404, 2014

[7] M. Drif, P. Perez, J. Aguilera, J. Aguilar, "A new estimation method of irradiance on a partially shaded PV generator in grid-connected photovoltaic systems," Renewable Energy **33** pp. 2048-2056, 2008

[8] S. Crocker, C. Sullivan, "Predicting Shading of Photovoltaic Systems with Cell-Level Resolution," IEEE Energy Conversion Congress and Expo (ECCE) 2013

[9] S. MacAlpine, C. Deline, R. Erickson, M. Brandemuehl, "Module mismatch loss and recoverable power in unshaded PV installations," 38th IEEE Photovoltaic Specialists Conference, 2012

[10] R. Levinson, H. Akbari, M. Pomerantz, S. Gupta, "Solar access of residential rooftops in four California cities," Solar Energy **83** pp 2120-2135, 2009

[11] N. Kukac, D. Zlaus, S. Seme et al., “Rating of roof’s surfaces regarding their solar potential and suitability for PV systems, based on LiDAR data,” Applied Energy **102** pp 803-812, 2013

[12] J.A. Jakubiec, C. Reinhart, “A method for predicting city-wide electricity gains from photovoltaic panels based on LiDAR and GIS data combined with hourly Daysim simulations,” Solar Energy **93** pp 127-143, 2013

[13] U. Jahn, W. Nasse, “Operational Performance of Grid-connected PV Systems on Buildings in Germany,” Progress in Photovoltaics **12**, pp. 441-448, 2004

[14] M. Gostein, R. Hershey, L. Dunn, B. Stueve, “Performance Analysis of Photovoltaic Installations in a Solar America City,” 34th IEEE Photovoltaic Specialists Conference, 2009

[15] A. De Benedictis, T. Hoff, S. Price, C. Woo, “Statistically adjusted engineering (SAE) modeling of metered roof-top photovoltaic (PV) output: California evidence,” Energy **35** pp. 4178-4183, 2010

[16] Tigo Energy, http://www.tigoenergy.com/content/academic-data-portal

[17] C. Deline, “Partially Shaded Operation of Multi-String Photovoltaic Systems,” 35th IEEE Photovoltaic Specialists Conference, Honolulu, HI, 2010.

[18] S. MacAlpine. R. Erickson, M. Brandemuehl, “Characterization of Power Optimizer Potential to Increase Energy Capture in Photovoltaic Systems Operating Under Nonuniform Conditions,” IEEE Transactions on Power Electronics **28** pp. 2936-2945, 2013

[19] B. Marion, et al. "Performance parameters for grid-connected PV systems," 31st IEEE Photovoltaic Specialists Conference, 2005.

[20] P Sharma, V Agarwal, “Maximum Power Extraction From a Partially Shaded PV Array Using Shunt-Series Compensation”, IEEE Journal of Photovoltaics 4 pp. 1128 - 1137, 2014

[21] J. Solórzano-Moral, D. Masa-Bote, M.A. Egido-Aguilera, & E. Caamaño-Martín, “A model for the simulation of energy gains when using distributed maximum power point tracking (DMPPT) in photovoltaic arrays.” Progress in Photovoltaics: Research and Applications. (2013)

[22] M. Mirjafari, R.S. Balog,, &R. Turan, (2014). Multiobjective Optimization of the DC--DC Stage of a Module-Integrated Inverter Based on an Efficiency Usage Model. IEEE JOURNAL OF PHOTOVOLTAICS, VOL. 4, NO. 3, MAY 2014

[23] M.S. Agamy, S. Chi, A. Elasser, M. Harfman-Todorovic, Y Jiang, F. Mueller, & F. Tao, A high-power-density dc–dc converter for distributed PV architectures. IEEE Journal of Photovoltaics, 3, 791-798. 2013

[24] C. Schaef and J. Stauth, “Multilevel Power-Point-Tracking for Partial-Power-Processing Photovoltaic Converters,” Emerging and Selected Topics in Power Electronics, IEEE Journal of, vol. 2, no. 3, Sept. 2014

[25] J.T. Stauth, M.D. Seeman, and K. Kesarwani, "A Resonant Switched-Capacitor IC and Embedded System for Sub-Module Photovoltaic Power Management," Solid-State Circuits, IEEE Journal of, vol.47, no.12, pp.3043,3054, Dec. 2012

[26] B. Burger, B. Goeldi, S. Rogalla, H. Schmidt, “Module Integrated Electronics – An Overview” 25th EU PVSEC Conference, 2010

**Alex J. Hanson** received the Bachelor of Engineering degree in electrical engineering with highest honors from the Thayer School of Engineering at Dartmouth, Hanover, NH in 2014. He is currently pursuing the Ph.D. degree in electrical engineering at the Massachusetts Institute of Technology, Cambridge, MA

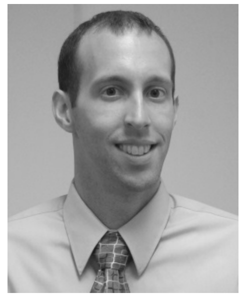

**Christopher A. Deline** (S’06-M’08) received the B.S., M.S., and Ph.D. degrees from the University of Michigan, Ann Arbor, in 2003, 2005, and 2008, respectively, all in electrical engineering. Since 2008 he has been a research engineer at the National Renewable Energy Laboratory in Golden, CO in the photovoltaic test and evaluation group. His research includes thin-film PV performance and stabilization, mismatch and partial shading in PV systems and distributed power electronics for PV.

**Sara M. MacAlpine** Sara M. MacAlpine received a Ph.D. degree in civil engineering from the University of Colorado at Boulder in 2014 and a B.S. degree in electrical engineering from Rice University, Houston, TX in 2001. Her research interests include photovoltaics, renewable energy systems, and building energy efficiency.

**Jason T. Stauth** (M’99) received his M.S. and PhD. degrees from the University of California, Berkeley in 2006 and 2008 respectively. In 2008, he co-founded QVSense, Inc., Berkeley, CA, where he worked on distributed power management for photovoltaic systems based on partial-power-processing architectures. Since 2011, he has been Assistant Professor at Dartmouth College, Hanover, NH. His research interests include highly integrated RF and power electronics for applications in renewable energy, transportation, and energy storage.

**Charles R. Sullivan** (SM’93–M’96–SM’12) received the B.S. degree in electrical engineering (with highest Hons.) from Princeton University, Princeton, NJ, in 1987, and the Ph.D. degree in electrical engineering from the University of California, Berkeley, in 1996.

He is currently an Associate Professor at the Thayer School of Engineering at Dartmouth, Hanover, NH. He worked for Lutron Electronics designing electronic ballasts. His research includes work on design optimization of magnetics for high frequency power conversion, thin-film magnetic materials and devices, and photovoltaic applications of power electronics. Dr. Sullivan has received the National Science Foundation Career Award and the Power Electronics Society Prize Paper Award.